Supplementary Information

Supplementary Figures

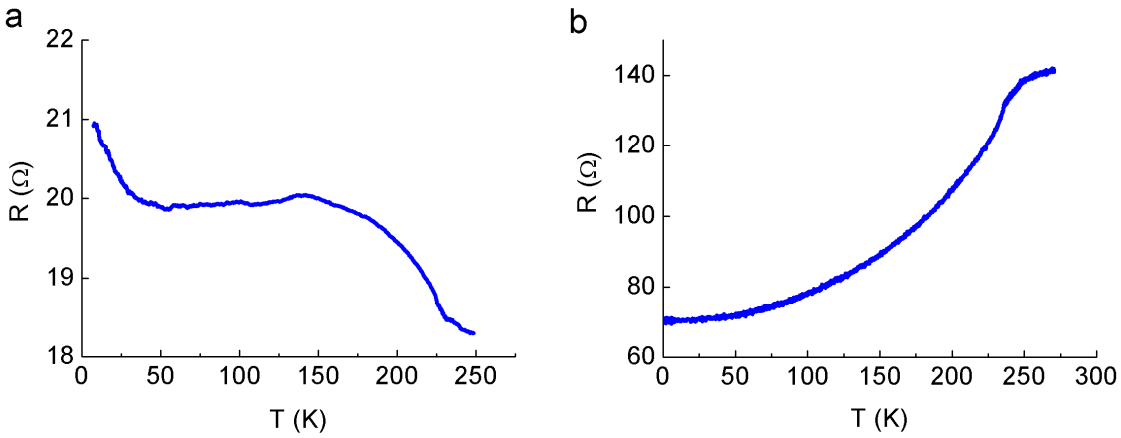

Supplementary Figure S1. Temperature dependence of the resistance of two different Bi_2Se_3 devices. One is 4 nm thick (a) and shows a weakly insulating behavior; the other (b) corresponds to the device whose data are shown in the main text: it is approximately 10 nm thick and it exhibits metallic behavior.

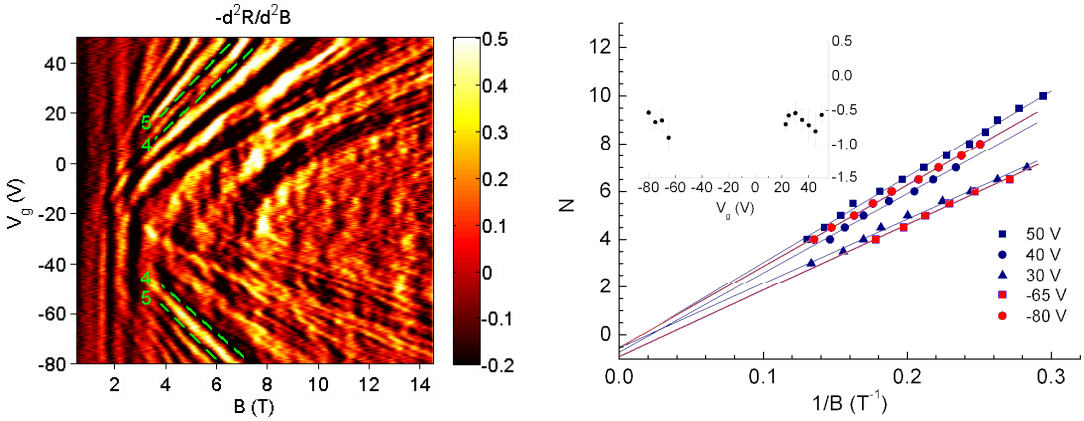

Supplementary Figure S2. Surface state Shubnikov-de Haas oscillations measured on a second device. Left panel: Fan diagram of Landau levels measured on a second device (the plot shows $-\frac{d^2R}{dB^2}(V_g, B)$). The overall behavior is identical to that of the device shown in the main text, exhibiting gate-dependent features fanning out from the charge neutrality point (which in this device is close to -20 V) and gate-independent features that originate from SdH oscillations due to carriers at the surface far away from the gate. At a quantitative level, the quality of the data is not as good as that of the measured data on the device discussed in the text, but a quantitative analysis of the "N-vs-1/B" relation is possible. This is shown in the right panel, for different values of gate voltage (when the gate voltage is close to the charge neutrality point, a quantitative analysis is not feasible, as discussed in the main text). Also in this case, the result is compatible with an extrapolated value of -0.5 and not of 0 (see inset). Note in the inset of the right panel that the points that deviate the most from -0.5 are also those on which the error -obtained from the linear fitting procedure- is the largest. Points for which the error is small are close to -0.5.

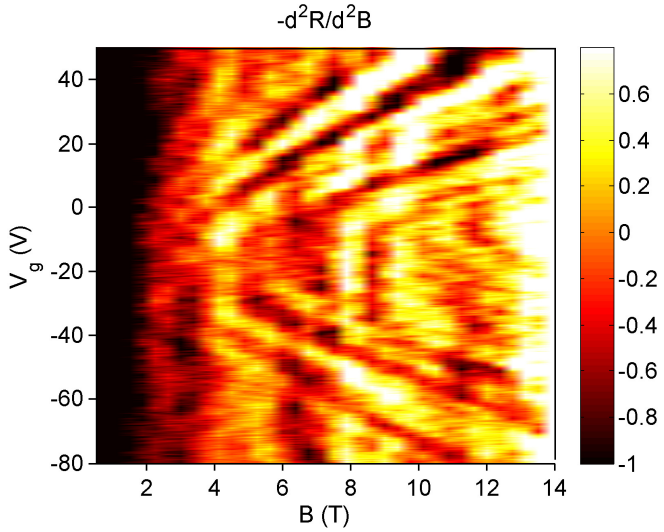

Supplementary Figure S3. Fan diagram measured on a third device. Both the dispersing, gate-dependent features and the "vertical" gate-independent features are clearly visible in the data, even though they are less pronounced as compared to the data measured in the device shown in the text and that shown in Supplementary Figure. S3. As a consequence (and also because the number of LLs that can be resolved is smaller), it is not possible to perform an accurate indexing of the levels on this device. Nevertheless, the data shown here represent an additional confirmation that the qualitative behavior observed in the other two devices is reproducible, and that the ambipolar transport and gate-tunable quantum resistance oscillations that we discuss are a robust phenomenon, commonly present in our devices.

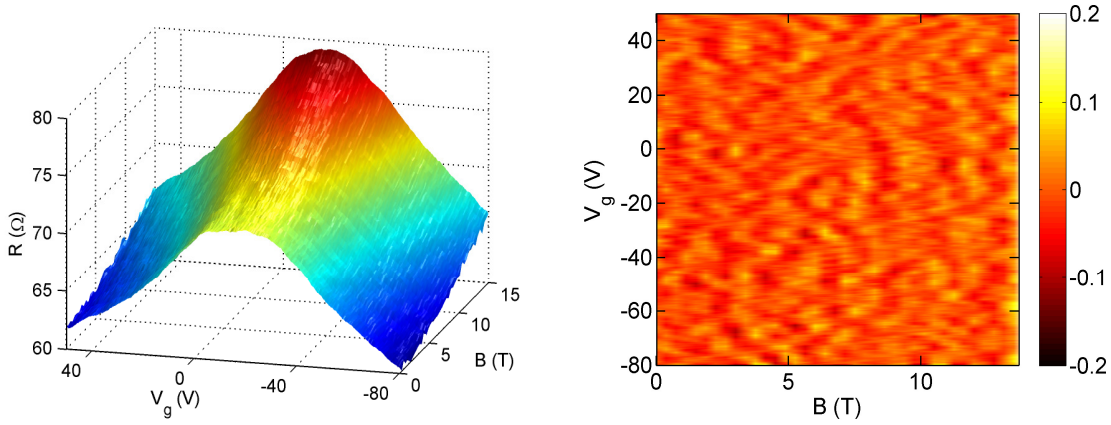

Supplementary Figure S4. Magnetoresistance in parallel magnetic field. The left panel shows the magnetoresistance as a function of gate voltage and in-plane magnetic field. It is apparent that the application of the magnetic field parallel –rather than perpendicular- to the crystal has only a small effect on the resistance. No fine features are present in this measurement. This is confirmed by taking the second derivative with respect to magnetic field (shown in the right panel), where only noise is seen.

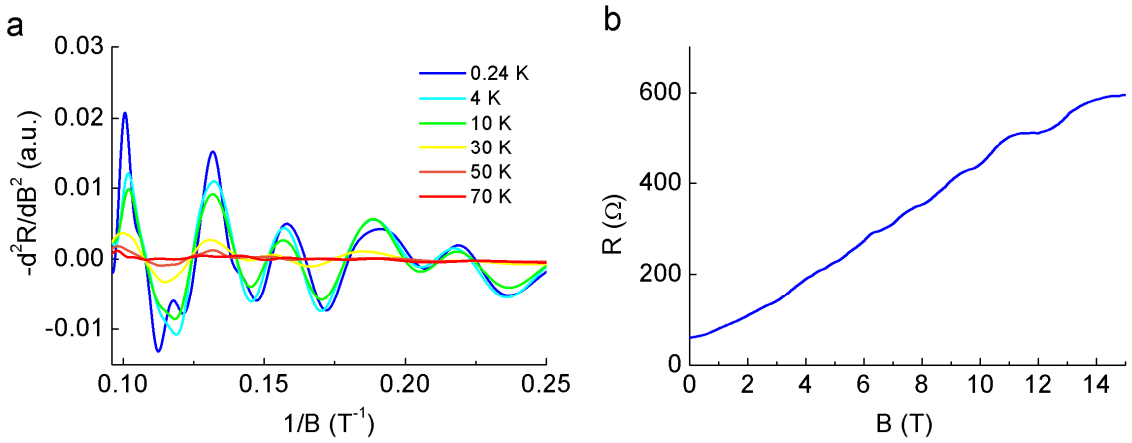

Supplementary Figure S5. **Temperature dependence of the magnetoresistance oscillations.** (a) Temperature dependence of the resistance oscillations observed in the second derivative of the resistance with respect to B (measured at V_g = 40 V). Despite the fact that oscillations remain visible up to fairly large temperature (as it can be expected, owing to the large energy spacing between LLs that is characteristic of Dirac fermions), their amplitude increases only slowly with lowering temperature. This is a consequence of the presence of the continuous density of states associated to the bulk impurity band. (b) Magnetoresistance measured at V_g = -80 V and T = 4.2 K. Note how at high magnetic field, the oscillations do resemble true plateaus: at these high field values, the analysis of SdH by looking at the derivative with respect to magnetic field starts not to be appropriate, because the effect of LLs cannot be any more thought of as that of small oscillations superimposed onto smooth background. That is why in Fig. 3a of the main text, features at high field are not sharply defined.

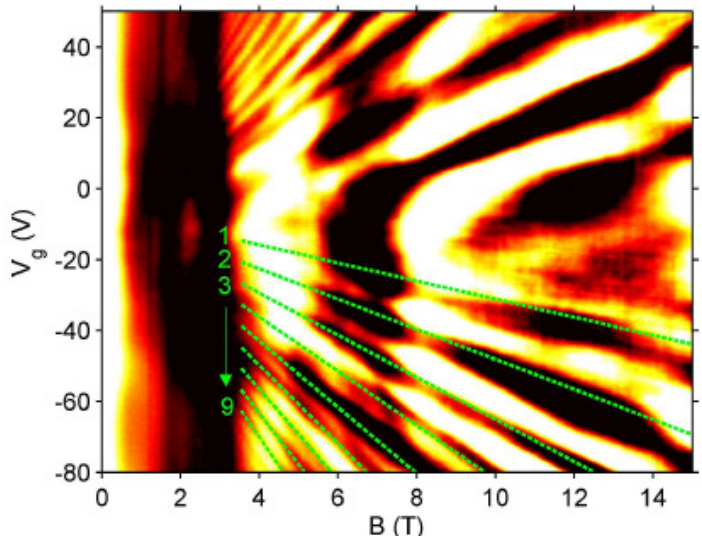

Supplementary Figure S6. Fan diagram obtained after background subtraction. Color plot of the measured magnetoresistance as a function of magnetic field B and gate voltage V_g, after subtracting a smooth background. The green dotted lines denote the position of the Landau levels (indexed by the corresponding numbers), as expected from the analysis of $-\frac{d^2R}{dB^2}(V_g, B)$ discussed in the main text. The good agreement with the position of the measured features shows that subtracting a background allows a correct analysis of the LLs. This analysis is particularly useful at high magnetic field, since it makes clearly apparent the LLs with N=1 and 2, which could not be identified in the color plot of $-\frac{d^2R}{dB^2}(V_g, B)$.

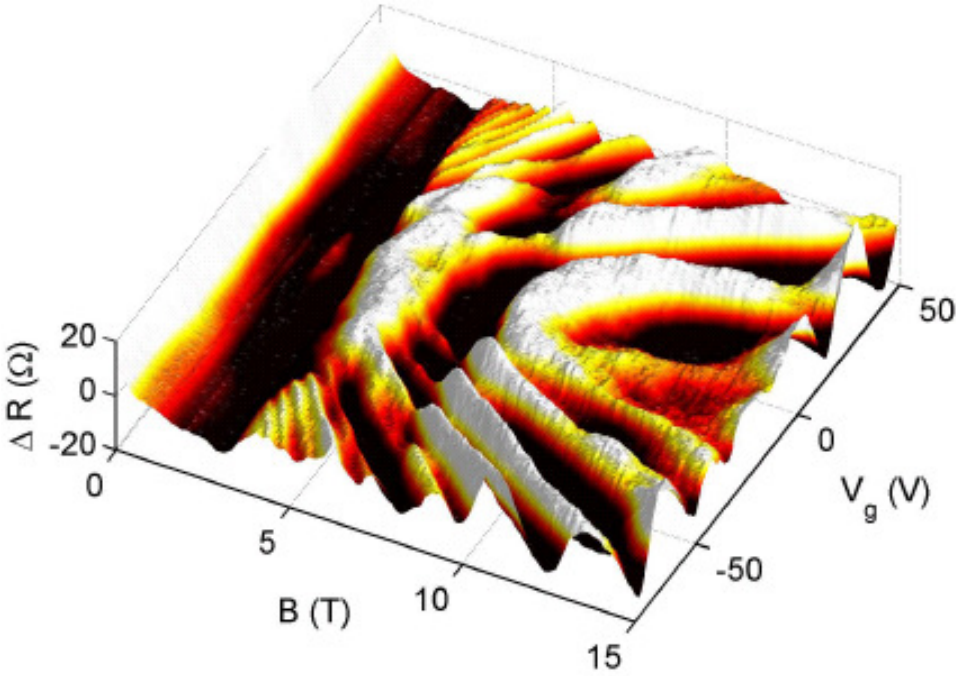

Supplementary Figure S7. 3D plot of the measured magnetoresistance as a function of magnetic field *B* and gate voltage V_g, after subtracting a smooth background. Next to the information that can also be extracted from the color plot of Supplementary Figure S6, the three dimensional plot illustrates how the amplitude of the features associated to the LLs increases for LLs with lower index.

Supplementary Notes

Supplementary Note 1

Data from other devices

For completeness, we show data from two additional devices that we measured, which exhibit the same behaviour that we have discussed in the main text. In both these two other devices, the fan diagram of Landau levels is clearly seen in the magnetoresistance measurements as a function of gate voltage and magnetic field. In particular, clear signatures of LLs due to electrons and holes dispersing in opposite directions, as the gate voltage is tuned across the charge neutrality point, are present (note that the position of the charge neutrality point in gate voltage is comparable in the different devices always ranging between -10 and -20 V) . Also in these devices the evolution as a function of gate voltage is continuous, pointing to the absence of a gap, consistently with the massless character of the carriers. For one of the devices (see Supplementary Figure S2) the quality of the data is sufficient to check the extrapolation of the N-vs-1/B plot and also in this case we find that the extrapolation is only compatible with "-1/2". For the other device (see Supplementary Figure S3), the number of LLs visible is not enough to perform a quantitative analysis of the LL indexing.

Together with the device whose data are shown in the main text, the two other devices discussed here show that: 1) ambipolar transport and SdH oscillations due to electrons and holes evolving smoothly as a function of gate voltage are present in several devices, 2) in all cases where we can index the LLs, the indexing is only compatible with massless Dirac fermions (as it should be expected from the absence of a gap in the fan diagram).

Supplementary Note 2

In-plane magnetoresistance.

When the magnetic field is applied in the plane of the Bi_2Se_3 crystals, no features are observed in the data. Supplementary Figure S4 shows that $-\frac{d^2R}{dB^2}(V_g, B)$ is indeed

completely featureless. This observation is consistent with a 2D behaviour of the electrons responsible for transport.

Supplementary Note 3

Background magnetoresistance

Here we discuss in detail several more technical aspects related to the analysis of our magnetoresistance measurements ($R(V_g, B)$), and to the analysis of the SdH effect by removing this positive magnetoresistance background. We emphasize that in the main text we have discussed the quantity $-\frac{d^2R}{dB^2}(V_g, B)$, because this quantity can be obtained directly from the experimental data without any "arbitrariness" that may be present in removing the background magnetoresistance. However, as we will show, removing the background is particularly useful to analyze the data at high magnetic field, and it allows to find clear features originating from Landau levels N=1 and 2, that are not easy to extract from the analysis of $-\frac{d^2R}{dB^2}(V_g, B)$.

As we have discussed in the main text, the measured magnetoresistance is due to the change in the conduction mediated by carriers in the impurity band[21], which can scatter in the states of the Landau Levels of the surface Dirac. This mechanism leads to a maximum in resistance when the Fermi level at the surface is in the middle of a Landau level and a resistance minimum when the Fermi level at the surface is in between two Landau levels (also in the two-terminal measurement configuration employed in our work). At low magnetic field, where the SdH effect starts to be visible, the modulation of the magneto-resistance is small, and the features can be well described as a sinusoidal oscillation superimposed on a background. Under these conditions, looking at the quantity $-\frac{d^2R}{dB^2}(V_g, B)$ provides an effective way to analyze the data. At higher magnetic field, however, the degeneracy of the Landau levels becomes larger and their effect leads to extended plateaus (see Supplementary Figure S5b, for instance). In this regime, the

features originating from LLs are not any more well described by sinusoidal oscillations superimposed on the positive background. To analyze the data at high field, we show here that features become visible after removing the positive magnetoresistance background (the presence of these features does not depend on the way in which the background is removed, which at most affect their precise position and sharpness). The data obtained after removing the positive magnetoresistance background are shown in the color plots in Supplementary Figure S6 and S7. It is apparent that the N=1 and N=2 Landau levels are clearly visible, at values of B and V_g in agreement with what is expected from the analysis performed on $-\frac{d^2R}{dB^2}(V_g, B)$. Note that, for the indexing of the Landau levels, it is in any case important to confine the analysis to small magnetic field range, in order to ensure that the Zeeman effect (which contributes to the opening of a gap, thereby suppressing the half-integer quantization) is negligible. A good indication for this is the presence of electron-hole symmetry in the Landau level filling, since the opening of a gap shifts the zero energy Landau level either in the conduction or the valence band and breaks this symmetry. In the range where we have analyzed $-\frac{d^2R}{dB^2}(V_g, B)$ as discussed in the main text, symmetric Landau level filling is rather well satisfied. At the largest fields reached in the experiment, violation of this symmetry starts to appear, indicating that these large magnetic fields should not be included in the analysis.

Finally, we comment on the presence of states in the impurity band with a continuous density of states, which coexist (at the same energy and overlapping in space) with the Landau levels. As discussed above, the electrons in the impurity band (which give a large contribution to transport in parallel to that of the surface Dirac electrons) are strongly hybridized with the surface states, which is why the formation of LLs affects the transport through the bulk. Therefore, contrary to the usual case where at sufficiently large B the Landau level separation becomes larger than their broadening, in the present case the Landau levels co-exist for all values of B with the continuous density of states in the impurity band. This has several consequences. For instance, it weakens the

temperature dependence of the Shubnikov-de Haas oscillations (as compared to the usual exponential dependence), which indeed we observe experimentally (see Supplementary Figure S5a). For Dirac fermions, whose LL energy scales proportionally to $B^{1/2}$, it also can affect the linearity of the fan diagram, since the added electrons do not have only to fill states in the Landau levels but also in the impurity band. We have checked with some simple numerical simulations that in the gate voltage range spanned in our experiments – and given the width of the features measured- this deviation from linearity is relevant only close to the charge neutrality point (where, however, LLs are not visible in the data). A consequence of the non linearity that can still be detected for $B \to 0$ is that the Landau levels of electrons and holes extrapolate to two slightly different (only a few Volts) values of gate voltage.

Supplementary Note 4

Different contributions to the normal state conductivity

To better understand the nature of transport in our Bi_2Se_3 devices, it is useful to analyze in some detail the conductivity at B=0, which originates from three contributions: the ones given by the two families of Dirac fermions on the opposite surfaces of the crystal, and that mediated by the carriers in the impurity band. For the Dirac fermions we write

$\sigma = n\, e\mu$

For the top surface n ~ 1.5 10^{15} m^{-2} (as obtained from the periodicity of the Shubnikov de Haas oscillations) is constant irrespective of the gate voltage, since the thickness of the Bi_2Se_3 crystal is larger than the electrostatic screening length (~3-4 nm). For the bottom surface n depends on V_g and can be varied through the charge neutrality point of the Dirac band. The conductivity of the impurity band is expressed in terms of the Einstein relation as:

$\sigma_{IB} = \nu^{2D}{}_{bulk} e^2 D$

where $\nu^{2D}{}_{bulk} = \nu_{bulk} t$ is the 2D density of states at the Fermi energy of impurity states, t is the thickness of the Bi_2Se_3 crystal, and D is the diffusion constant of the carriers. With varying the gate voltage, the Fermi energy in the impurity band shifts, but since ν_{bulk} is

approximately constant, σ_{IB} does not change significantly. As a result, the gate voltage mainly affects the conductivity of the Dirac fermions located on the surface closest to the gate electrode.

At B=0, the total conductivity is

$$\sigma_{Total} = G\frac{L}{W} = 1.79\ 10^{-3}\ \text{S}$$

where L is the separation between the contacts and W is the sample width (in the geometry of our device we could measure the contact resistance directly: we found it to be negligibly small, ~2-3 Ω). The conductivity of the top surface Dirac fermions (σ_{TS}) estimated from the values of n and μ (5000 cm^2/Vs) extracted from the magnetoresistance measurements is

$$\sigma_{TS} = 1.2\ 10^{-4}\ \text{S}$$

At the charge neutrality point, the conductivity at the bottom surface can be neglected as compared to that of the top surface, because of the lower carrier density and lower mobility. Therefore we obtain:

$$\sigma_{IB} = 1.6\ 10^{-3}\ \text{S}.$$

This is one order of magnitude larger than the contribution given by the Dirac fermions even at the largest gate voltage reached in the experiments. The properties of Dirac electrons can nevertheless be clearly observed thanks to their sensitivity to the magnetic field and –for the bottom surface- to the gate voltage, as described in the main text. Knowing the density of states in the impurity band (see main text), we extract the diffusion constant of carriers in the impurity band to be

$$D_{IB} \approx 1.5\ 10^{-2}\ \text{m}^2/\text{s}.$$

Interestingly, the diffusion constant of the Dirac electrons on the top surface coincide (given the approximations involved in our estimates) with this value:

$$D_{TS} = \frac{1}{2}v_F^2\tau = \frac{\hbar k_F v_F \mu}{2e} \approx 1.1\ 10^{-2}\ \text{m}^2/\text{s}.$$

This finding indicates –as we have mentioned in the text- that the diffusion of carriers in the impurity band occurs largely through their coupling to the Dirac surface states, which

is strong since the crystal thickness is comparable to the Bohr radius of the impurity states (the same coupling is likely to be the dominant factor limiting the mobility of the Dirac fermions). This is also the reason why the contribution of the conductance of the impurity band is strongly affected by a perpendicular magnetic field which causes the formation of LLs at the surface, since through the coupling between impurity band and surface states, the diffusion of the electrons in the impurity band is affected.

As a final remark, we note that it is very interesting that the Dirac surface fermions preserve their character despite the presence of a large density of states at the same energy, which overlap in space. This robustness of surface states is not only characteristic of our experiments, but has been observed more in general, for instance in ARPES experiments. In that case, it has been found that in crystals where the Fermi level is in the conduction band, surface states (evolving continuously from the Dirac fermion states in the gap) are still present and remain well defined. Also theoretically, surface states have been seen to be robust against the presence of bulk states at the same energy[38].

Supplementary Note 5

Relation between gate voltage and density of Dirac electrons

In the presence of the states in the impurity band, the density of Dirac electrons that is accumulated on the bottom surface upon varying the gate voltage, $n_{Dirac}(V_g)$, is significantly smaller that the total density of accumulated charge $n_{Tot} = \frac{C\left|V_g - V_g^{CN}\right|}{e}$. To find the relation between $n_{Dirac}(V_g)$ and $n_{Tot}(V_g)$, we imagine to vary V_g starting from the charge neutrality point, and we impose that, in equilibrium, the highest occupied states in the Dirac surface band and in the bulk impurity band have the same energy E_F. In terms of the density of states of the Dirac electrons and of the impurity band we have:

$$n_{Tot}(V_g) = n_{IB}(V_g) + n_{Dirac}(V_g) = \nu_{Bulk}\lambda_{TF}E_F + \frac{1}{4\pi}\frac{{E_F}^2}{(\hbar\, v_F)^2},$$

where we consider that the charge is accumulated over a depth λ_{TF} (Thomas-Fermi screening length) from the surface. We solve this equation for E_F as a function of $n_{Tot}(V_g)$ and insert the value found in the expression for the density of Dirac fermions to obtain:

$$n_{Dirac}(V_g) = \frac{1}{4\pi}\frac{{E_F}^2}{(\hbar\, v_F)^2} = \pi(\hbar\, v_F)^2\left[-\nu_{Bulk}\lambda_{TF} + \sqrt{(\nu_{Bulk}\lambda_{TF})^2 + \frac{n_{Tot}(V_g)}{\pi(\hbar\, v_F)^2}}\right]^2,$$

which is the equation written in the main text. It follows from this expression that the presence of the density of states in the impurity band largely suppresses (for the value of ν_{Bulk} in our Bi_2Se_3 crystals, which compares well to literature estimates[21], see main text) the amount of charge accumulated in the Dirac states, as compared to what is expected from the geometrical capacitance. This is what we observe in the fan diagram originating from the filling of Landau levels.

Supplementary References

38. Bergman, D.L. and Refael, G. Bulk metals with helical surface states. *Phys. Rev. B* **82,** 195417 (2010).